Vaccine 37 (2019) 903–909

Contents lists available at ScienceDirect

Vaccine

journal homepage: www.elsevier.com/locate/vaccine

Short communication

Novel IFN-γ ELISpot reveals robust T cell responses elicited after influenza nucleoprotein DNA vaccination in New Zealand White rabbits

Bryan S. Yung [a], Holly Pugh [a], Alison A. Generotti [a], Nikki Phanhthilath [a], Katherine Schultheis [a], Kar Muthumani [b], Kate E. Broderick [a], Trevor R.F. Smith [a,*]

[a] Inovio Pharmaceuticals Inc, San Diego, CA, USA
[b] Vaccine & Immunotherapy Center, Wistar Institute, Philadelphia, PA, USA

ARTICLE INFO

Article history:
Received 11 September 2018
Received in revised form 3 January 2019
Accepted 5 January 2019
Available online 17 January 2019

Keywords:
DNA vaccine
T cell
Rabbit
ELISpot

ABSTRACT

The New Zealand White rabbit is a highly accessible animal model which is regularly employed in biomedical research. However, the paucity of rabbit-specific reagents available limits its use in certain fields. Specifically, the lack of a reliable T cell assay has limited its employment in immune prophylactic and therapeutic studies. To address this inadequacy, we have developed an ELISpot assay to detect cellular immune responses (IFN-γ production) after antigenic stimulation. We have applied this assay to model the T cell responses elicited by a DNA vaccine. Immunization with an influenza nucleoprotein (NP) DNA vaccine revealed strong antigen-specific T cell responses in the peripheral blood mononuclear cell population. We believe this is the first report of such an assay in rabbit species, and it will become a useful tool to monitor *in vivo* responses to vaccines and permit the wider adoption of this model to measure immunological responses.

1. Introduction

The rabbit (*Oryctolagus cuniculus*) is a valuable research model for biomedical and pharmaceutical research. In recent years, it has become the choice bioreactor for the production of monoclonal and polyclonal antibodies as well as recombinant proteins [1,2]. The biological response in rabbits to drugs and diseases is similar to that observed in humans, and advancements in rabbit genomics and proteomics have positioned the New Zealand White (NZW) rabbit as the model of choice for translational medicine research in many disease areas, including cardiovascular disease [3,4], ocular cancer [5,6], and infectious diseases [7,8]. Importantly, rabbits are phylogenically closer to primates than rodents [9] and do not present the significant financial and ethical burden which is involved with the employment of pigs, canines and non-human primates as experimental models. For many pre-clinical and translational medicine programs, the rabbit could offer a viable replacement or intermediary to these other large animal models. For example, we have employed the NZW as a surrogate model for assessing clinically relevant drug delivery protocols of immune prophylactics and therapeutics. However, the scarcity of immunological reagents available to measure cellular responses in rabbits has greatly limited the advantages of this animal model for vaccine development. Currently, vaccine development in the rabbit model has largely been restricted to measuring humoral responses, which alone is not necessarily indicative of relevance of the vaccine elicited immune response to many disease targets [10,11].

In response to this inadequacy we investigated the potential of an Enzyme-Linked ImmunoSpot (ELISpot) assay to detect interferon gamma (IFN-γ) secretion for PBMCs to monitor cellular immune responses in NZW rabbits vaccinated with a plasmid DNA (pDNA) vaccine. The ELISpot is a qualitative and quantitative assay that has been developed as a routine assay to monitor cell-mediated immunity by enumerating antigen-specific T or B cells producing IFN-γ. IFN-γ is a cytokine produced by primarily by CD4 + T-helper 1 effector cells and CD8 + T lymphocytes. It plays an important role in directing protection against intracellular pathogens by activating and supporting natural killer cells, macrophages, and cytotoxic T cells, as well as up-regulating antigen presenting molecules, immunoglobulin class switching in B cells, and generating antitumor T cells [12–17]. As such, the ability to measure IFN-γ responses is an invaluable tool in determining the generation of strong T cell responses against a particular antigen and vaccine potency. IFN-γ production by T cells has been associated with protection against many viruses, including influenza

* Corresponding author at: Inovio Pharmaceuticals, 10480 Wateridge Circle, San Diego, CA 92121, USA.
E-mail address: tsmith@inovio.com (T.R.F. Smith).

https://doi.org/10.1016/j.vaccine.2019.01.006
0264-410X/

[18,19]. T cell IFN-γ responses have also correlated with influenza vaccine efficacy in human populations [20,21].

Here we delineate the development of the IFN-γ ELISpot to detect T cell responses in rabbits using a pair of commercially available capture and detection antibodies. We demonstrate the rabbit IFN-γ ELISpot assay's ability to quantify and examine cell-mediated responses in the NZW rabbit after a series of vaccinations against the influenza-A nucleoprotein (NP), as well as respiratory syncytial virus (RSV) antigens. The sensitivity of the optimized assay allowed us to examine prime and boost strategies against both vaccines from lymphocytes isolated from peripheral blood mononuclear cells (PBMCs) as well as detectable dose responses between different vaccines. The utilization of this assay to characterize T cell responses following DNA vaccination lends a greater insight into the rabbit model as a viable animal model for translating preclinical vaccine development into the clinic. The results further support the advancement of T cell stimulating universal influenza DNA vaccines designed to target the conserved internal antigens such as NP.

2. Materials and methods

2.1. Animals

Ten- to twelve-week-old female New Zealand White rabbits were purchased from Charles River Laboratories (Wilmington, MA). Animals were singlehoused with *ad libitum* access to food and water and handled at Acculab (San Diego, CA) according to the standards of the Institutional Animal Care and Use Committee (IACUC).

2.2. Animal treatments

Rabbits were placed in an induction chamber and anaesthetized at 5% isoflurane vapor. Animals were then removed from the chamber and anesthesia was maintained by 2% isoflurane vapor delivered through a nose cone. Hind legs of the rabbits were shaved and disinfected with ethanol prep pads. A 3 mL syringe with a 21G2 needle was used to deliver the 1 mL pDNA formulation into the quadriceps. Intramuscular (IM) electroporation was performed immediately after injection using the CELLECTRA® 2000 device, which delivers three pulses, at a constant current of 0.5 A, through an array composed of 5 needles. Each pulse is 52 msec in duration with a 198 msec interval between each pulse.

2.3. Plasmid DNA

The influenza nucleoprotein plasmid vaccine (pNP) encodes the full-length NP derived from the A/Puerto Rico/8 (H1N1) strain of the influenza A virus. The RSV-F plasmid vaccine (pRSV-F) contains a consensus sequence of the RSV fusion glycoprotein of subtype A and B viruses.

2.4. Overlapping peptide pools

Overlapping peptide pools for the influenza A virus (A/Puerto Rico/8/34(H1N1)) nucleoprotein were created by generating 120 individual 15 mer peptides spanning the 498 amino acid antigen sequence (Supplementary Fig. 1). The RSV-F peptide pool was matched to the consensus sequence of the RSV fusion glycoprotein of subtype A and B viruses (Supplementary Fig. 2). For both NP and RSV-F antigens the peptides overlapped by 11 amino acids, creating a 4 amino acid shift between subsequent peptides. Peptides for influenza A viruses NP were then split into three pools, each containing 40 peptides. RSV-F peptides were split into four pools of 20 peptides.

2.5. Animal sampling and PBMC processing

Five mLs of peripheral blood was drawn from the central ear artery of each rabbit using a 10 mL syringe and immediately transferred into either CPT (BD Biosciences, San Jose, CA) or K2EDTA spray-coated (BD Biosciences, San Jose, CA) blood collection tubes. Blood was diluted 1:2 with Hank's Balanced Salt Solution (Gibco, Waltham, MA) and layered over a Ficoll-Paque Plus density gradient (GE Healthcare Life Sciences, Pittsburgh, PA) in a SepMate-15 tube (STEMCELL, Vancouver, BC) and centrifuged at 1200*g* for 10 min at ambient temperature. PBMCs were isolated and red blood cell contamination was removed by ACK lysis. Cell are then enumerated by trypan blue staining and re-suspended at 2×10^6 viable cells/ml in R10 medium (10% fetal bovine serum (FBS), 1% Penicillin/Streptomycin, and 0.1% beta-mercaptoethanol in RPMI medium).

2.6. Rabbit IFN-γ ELISpot assay

96-well MultiScreen IP plates (EMD Millipore, Burlington, MA) were coated with 15 μg/ml primary anti-rabbit IFN-γ monoclonal antibody MT327 (Mabtech, Nacka Strand, Sweden) and blocked with R10 medium. 100 μl of peptide pools, PMA/ionomycin (0.4 μg/ml and 4 μg/ml, respectively (Sigma Aldrcih, St. Louis, MA)), ConA (2.5 μg/ml (Sigma Aldrich)), or R10 were added to the plates. Cells were then plated at 200,000 cells/well in 100 μl, with experimental conditions assayed in triplicates, or at 25,000 cells/well in 100 μl for the mitogen positive control to prevent spot confluency. After an 18 h incubation in a humidified 5% CO_2, 37 °C incubator, cells were removed by washing with PBS and 100 μl of 0.1 μg/ml biotinylated anti-rabbit IFN-γ monoclonal antibody MT318 (Mabtech) in a 0.5% FBS-PBS solution was added. After a 2 h incubation and washing, 100 μl of alkaline phosphatase-conjugated streptavidin (Mabtech) was added to each well for 1 h. Following washes, 100 μl of BCIP/NBT detection reagent substrate (Mabtech) was added to each well, and plates were incubated in the dark for 10 min. IFN-γ positive spots were imaged, analyzed, and counted using a CTL-Immunospot S6 ELISpot plate reader (Cleveland, OH) and CTL-Immunospot software.

2.7. Endpoint-binding titer ELISA

Antibody responses against NP and RSV were evaluated by ELISA using serum from immunized rabbits. Thermo Fisher Scientific Nunc High-Binding 96 well assay plates (Thermo Fisher, Waltham, MA) were coated with 100 μl per well of 0.3 μg/ml of either Influenza A H1N1 nucleoprotein or human respiratory syncytial virus (A2) fusion glycoprotein (Sino Biological, Beijing, China) and incubated overnight at 4 °C. Unbound antigens were washed by automated plate washing with 0.05% Tween-20 PBS. The plates were blocked to prevent downstream non-specific protein binding with 250 μl of 0.5% bovine serum albumin (BSA) for 1 h at 37 °C. Plates were washed as described above. Serum was diluted 1:50 in PBS with 0.2% BSA and 0.05% Tween-20 and added to the first row of the plate. Serial dilutions of 1:3 from the first row down were made for each sample in the plate. The serially-diluted serum was incubated for 2 h at 37 °C before washing. Goat anti-rabbit HRP-conjugated detection antibody (Jackson ImmunoResearch Laboratories, West Grove, PA) was diluted 1:10,000 and added to the plates, followed by a 1 h incubation at 37 °C. After washing, plates were developed using 100 μl per well of SureBlue™ TMB 1-component (Seracare, Milford, MA) and incubated for 10 min. 100 μl of TMB Stop Solution (Seracare) was then added to stop

the reaction. Optical densities were read at 450 nm and the end point titer was determined as the last serial dilution which produced an OD two times greater than that of background control.

3. Results

3.1. Optimization of processing and mitogenic stimulation of rabbit PBMCs

For ELISpot assay optimization, experiments were performed to maximize PBMC recovery and viability, and to examine positive control readouts for assay sensitivity. Whole blood samples from pNP vaccinated rabbits were divided into either K2EDTA or CPT blood collection tubes. PBMCs were processed according to manufacturer specifications or as described in the methods section. Cells were then enumerated by trypan blue viability staining and the total viable cell count and percent viability were measured (Fig. 1A). We were able to obtain an average of 5×10^6 viable PBMCs from 5 mLs of peripheral blood collected from the ear artery with an average percent viability of 85 percent. Cells were then stimulated for 18 h with NP peptide pool 1 to assess possible variations in responses that may be caused by cell quality (Fig. 1B). Although there is no significant difference in total viable PBMCs or in percent viability of cells using either isolation method, IFN-γ positive SFU development was significantly different between the two methods, with mean response of 545 SFUs/10^6 from the K2EDTA-based method compared to 31 SFUs/10^6 from the CPT-based method. To determine an appropriate positive readout for the ELISpot assay, mitogenic stimulation of PBMCs with concanavilin A (ConA) and phorbol myristate acetate/ionomycin (PMA/I) were used, with PMA/I generating an overall greater mean IFN-γ response of 17,470 SFUs/10^6 compared to 1511 SFUs/10^6 from ConA (Fig. 1C). As a result, PMA/I was used in all future assays as a positive readout due to its ability to robustly stimulate IFN-γ responses.

3.2. Detection of IFN-γ + lymphocytes following influenza NP DNA vaccination of rabbits

To assess antigen-specific T cell responses, we immunized five NZW rabbits with 100 μg of a pNP DNA on day 1 and 14. Prior to immunization rabbits were prescreened for NP-reactive antibodies, and no influenza sera-conversion was detected. The pNP vaccine had previously been shown to elicit robust T cell responses in other laboratory animals including mice [22], guinea pigs [23], and nonhuman primates [24]. To confirm that the rabbits had developed immune responses against the influenza NP antigen following the two vaccinations, we collected serum and analyzed for antibody binding titers on day 26 (Fig. 2A). All immunized rabbits were seroconverted after two vaccinations and developed IgG antibodies binding the NP antigen. To evaluate cell-mediated responses against influenza NP, PBMCs were isolated from whole blood from treated and untreated rabbits. Cells were plated onto ELISpot wells coated with anti-rabbit IFN-γ capture antibody and stimulated with influenza NP peptide pools containing 15mer peptides spanning the entire influenza NP-PR8 recombinant protein encoded by the pDNA vaccine. Representative well images for each of the treated rabbits and one untreated rabbit are represented in Fig. 2B, with a medium, negative control group and three peptide pool stimulated groups. IFN-γ positive spot forming units (SFU) in each well were enumerated and calculated per million cells for both treated and untreated rabbits. For the pNP-treated rabbits, no particular peptide pool dominated over another after the two immunizations; mean spot counts for peptide 1, 2 and 3 were 551, 483, and 517 SFUs/10^6 cells, respectively (Fig. 2C). In the

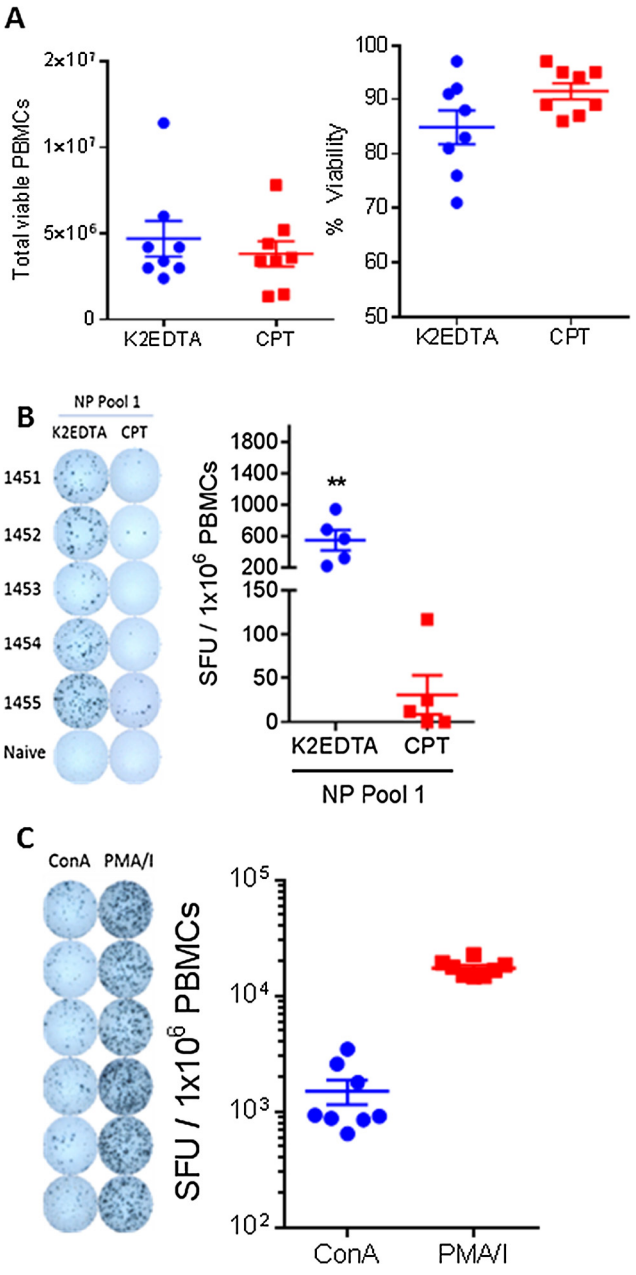

Fig. 1. Optimization of blood sampling and isolation of peripheral blood mononuclear cells from New Zealand White rabbits immunized with 100 μg of DNA vaccine encoding the influenza virus PR8 nucleoprotein (pNP). (A) PBMCs were isolated from 5 mLs of blood collected in either K2EDTA-spray coated or CPT tubes. Total viable cell counts and percent viability were determined with trypan blue staining and enumerated. Reported as mean ± SEM. (B) Representative image of the comparison between PBMCs isolated from K2EDTA tubes vs CPT tubes after overnight stimulation with peptide pool 1 in wells coated with anti-rabbit IFN-γ capture antibody. IFN-γ + SFUs were detected and enumerated after stimulation with NP peptide pool 1 in pNP-immunized (Animal ID: 1451–1455) and non-treated rabbits. The mean SFU ± SEM for pool 1 is displayed ($^{**}P < 0.01$). (C) Representative images of spot development after stimulation of PBMCs with ConA and PMA/ionomycin and enumeration of IFN-γ + SFUs. Mean SFUs ± SEM are plotted ($^{***}P < 0.001$).

untreated rabbits, the response to the peptide pools were not significantly higher than the background levels depicted in the medium control wells (Fig. 2B). The IFN-γ ELISpot readout in response to stimulation with the peptide pools spanning the influenza NP antigen averaged 1552 SFUs/10^6 PBMCs across the animals in the

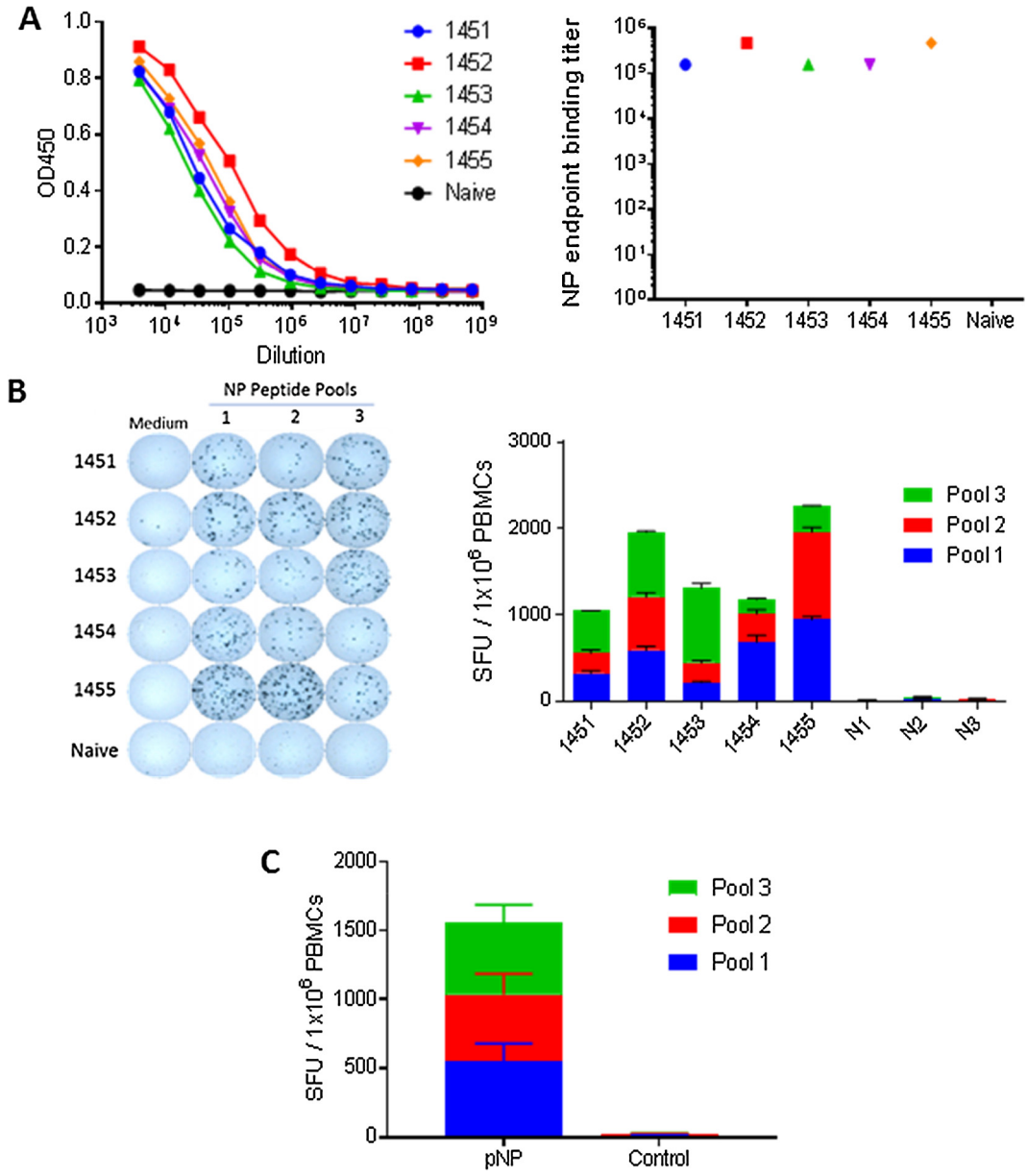

Fig. 2. Robust humoral and IFN-γ + cellular immune responses are detected after 100 μg pNP immunization. On days 1 and 14, pNP was delivered IM with electroporation. (A) Anti-influenza PR8 nucleoprotein binding curves and endpoint binding titers were detected in the serum of pNP-immunized rabbits by ELISA. The IFN-γ ELISpot response to NP peptide pools 1–3 was measured on day 26, 12 days after the boost immunization. (B) Representative well images of an IFN-γ ELISpot response of five pNP-immunized and one untreated (naïve) rabbit. Individual IFN-γ + cellular responses were then enumerated and plotted (mean SFU ± SEM). (C) The average SFU's for each pool in the pNP-immunized group compared to the non-treated group is displayed.

pNP vaccine group compared to 32 SFUs/10^6 PBMCs across the untreated rabbits.

3.3. Kinetics of cell-mediated responses by pDNA vaccines measured by IFN-γ ELISpot in rabbits

The development and optimization of this rabbit ELISpot allowed us to monitor the cellular immune response to determine the efficacy of our pDNA vaccine delivery and electroporation protocols. The ability to measure the strength of the immune response after each immunization in a vaccination regimen can provide a better understanding in the pharmacokinetics of vaccine-induced cellular responses. To investigate the development of the host immune response to NP antigen during a vaccination regimen we assessed the IFN-γ response in PBMCs after 1 and 2 immunizations.

We delivered 50 μg of pNP intramuscularly in nine New Zealand white rabbits in combination with electroporation with the CELLECTRA®-5P EP device on day 1 and day 21. IFN-γ ELISpot and humoral responses were measured two weeks after each immunization and presented in Fig. 3A, 3B, and 3C. Fig. 3A displays the IFN-γ ELISpot cellular immune response kinetics to the influenza NP peptide pool 1–3 and Fig. 3B displays group responses to each individual peptide pool at each time point. Strong IFN-γ responses were observed 2 weeks after the first immunization, averaging 735 SFUs/10^6. Significantly increased IFN-γ SFU's were enumerated after the second vaccination (2600 SFUs/10^6). Immune responses against the antigenic determinants of the influenza NP were broad and spanned all peptide pools evenly after the prime; 30.4%, 37.4%, and 32.2% of the total IFN-γ response was directed towards pools 1, 2 and 3 respectively (Fig. 3B). There was no dom-

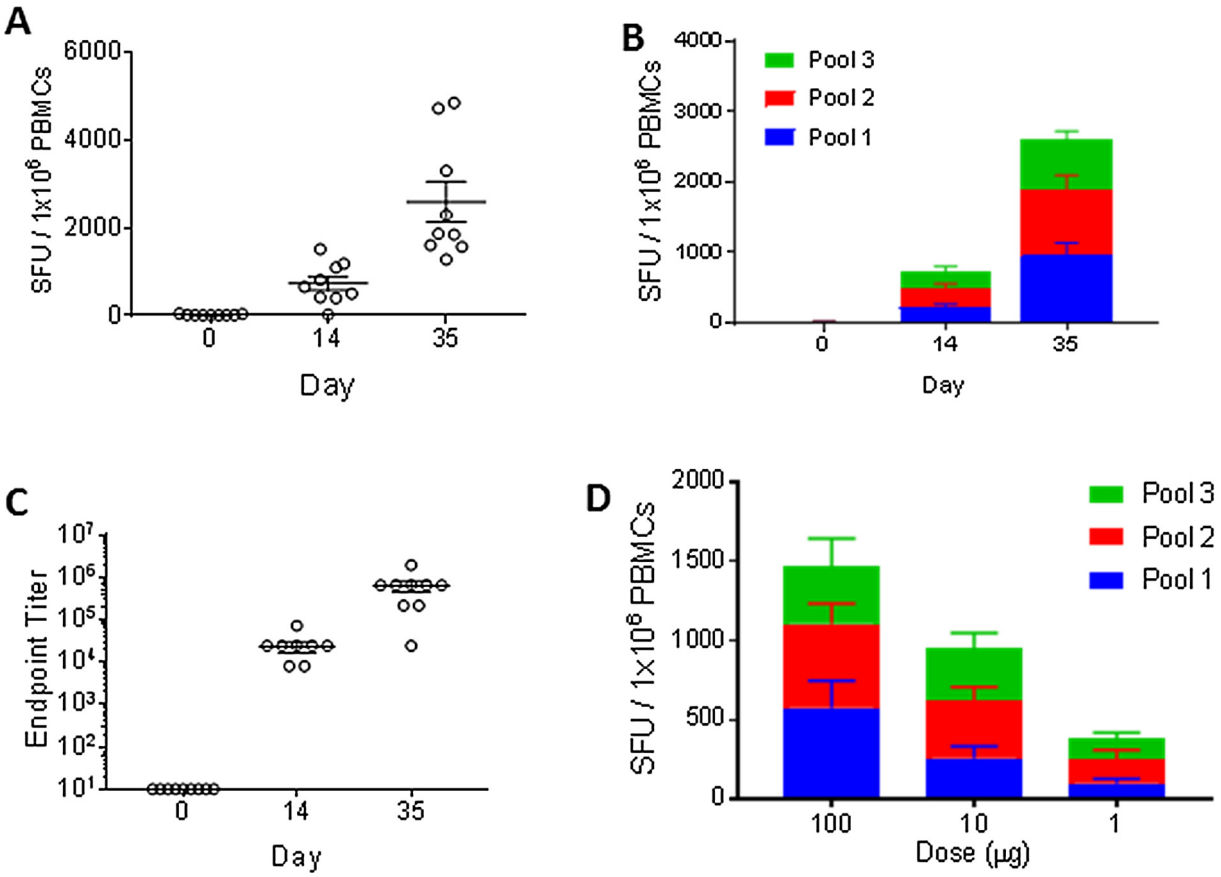

Fig. 3. Kinetics of cellular immune response elicited by pNP vaccine regimen measured by IFN-γ ELISpot. (A) 9 rabbits were immunized with 50 μg of pNP with IM electroporation on days 1 and 21. The PMBC IFN-γ ELISpot response was measured before treatment to determine baseline, 14 days after the prime (day 14), and 14 days after the boost (day 35). Mean SFU ± SEM are plotted for each animal. (B) IFN-γ ELISpot responses to each peptide pool on day 1, day 14, and day 35 are summarized. (C) Anti-influenza PR8 NP antibody responses from each animal are measured by endpoint binding titer (mean ± SEM). (D) 15 rabbits (5 per group) were dosed with either 100, 10, or 1 μg of pNP on day 1. On day 14, PBMCs from treated rabbits were stimulated with NP peptide pools 1–3 and their IFN-γ + SFUs were enumerated. Mean responses ± SEM from each group to each peptide pool are displayed.

inant response against a particular peptide pool determinant after the second effect was measured (36.6% for pool 1, 35.8% for pool 2, and 27.6% for pool 3), indicating a broad T cell response against multiple NP antigenic determinants had been raised. Binding titers against influenza NP were also measured and reflected boosting in humoral responses, to support the observations demonstrated by the cell-mediated responses (Fig. 3C). Mean endpoint binding titers after the prime were 1:23, 400 and after the boost were 1:634, 500.

To characterize rabbit immune responses to antigen dose, New Zealand White rabbits were dosed with either 100, 10, or 1 μg of pNP and their responses were measured by IFN-γ ELISpot two weeks post-treatment. As expected, we were able to observe a dose response curve with the pNP (Fig. 3D). Rabbits treated with a single treatment of 100 μg had a cumulative mean response of 1470 SFUs/10^6. With each ten-fold reduction of dose, animals had a group average response of 956 and 380 SFUs/10^6 for 10 and 1 μg, respectively.

3.4. Detection of cellular responses to RSV vaccine

To investigate the versatility of the assay we assessed IFN-γ responses elicited by vaccine against a different infectious disease target: RSV-F [23]. We analyzed antigen-specific responses in rabbits immunized with pRSV-F. Five naïve NWZ rabbits were dosed with 200 μg of pRSV-F on day 0 and 21, and the IFN-γ responses and anti-RSV-F antigen-antibody binding titers were measured two weeks after each immunization. Analysis of the response to the four RSV-F peptide pools are displayed in Fig. 4B as total average spot counts for each time point. The prime response at day 14 was a mean value of 160 SFUs/10^6, with an almost two-fold increase to 313 SFUs/10^6 after the second dose. The kinetics of the cell-mediated immune response reflected the humoral response against the RSV-F antigen, where a clear boosting in antibody responses was observed after the second immunization (Fig. 4A). In summary, we have demonstrated the ability of DNA vaccines targeting a variety of antigens to elicit cellular immune responses using a newly available rabbit IFN-γ ELISpot assay.

4. Discussion

For the rapid preclinical development of our pDNA vaccine candidates, it was essential to develop a highly accessible large animal model. The rabbit model provides an appropriate body size and muscle mass, unlike small rodents, which is compatible with IM-Electroporation drug delivery platforms design for clinical use, without the high ethical and housing costs of non-human primates. With the ongoing development of rabbit-specific reagents, the value of the rabbit as an experimental model in translational research will appreciate.

To advance the value of the rabbit as an important experimental model to measure immunity we developed and optimized an IFN-γ ELISpot to measure T cell response to antigenic determinants. As reported here, optimizations to non-terminal blood sampling to isolate and process a substantial amount of peripheral T cells

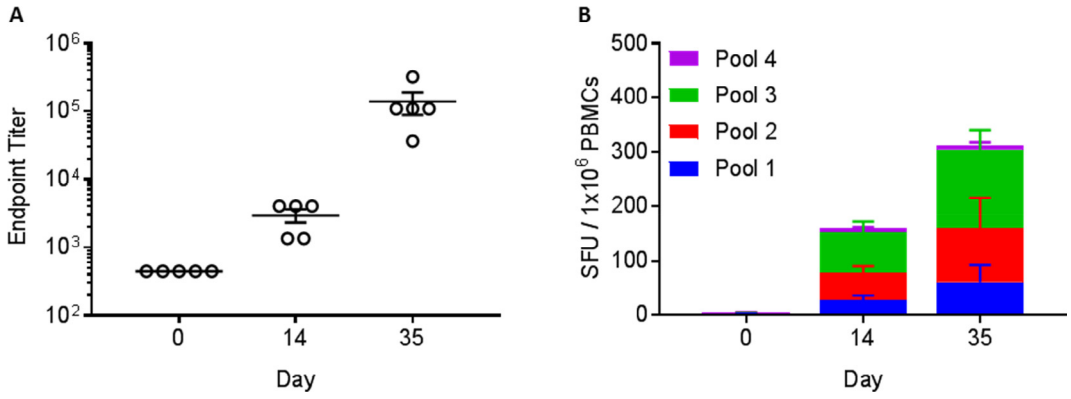

Fig. 4. IFN-γ + ELISpot responses are detected in rabbits immunized with pRSV-F. 5 rabbits were immunized with 200 μg of pRSV-F (delivered IM with electroporation) on day 1 and 21. (A) Serum was collected on days 0, 14, and 35 and anti-RSV-F antibody responses from each animal were measured by endpoint binding titers (mean ± SEM). (B) PBMCs were isolated on days 0, 14, and 35 and stimulated overnight with peptide pools 1–4 spanning the fusion glycoprotein consensus sequence for virus subtypes A and B. For each assessment date, mean SFUs ± SEM to each peptide pool are plotted.

allows clear enumeration of IFN-γ positive spot forming units upon stimulation with antigenic peptides. The added benefit of non-terminal sampling permits repeat immunizations, which is invaluable in assessing vaccine immunogenicity and duration T cell immunity across treatment regimens. An important observation in the assay concerned the processing of the whole blood samples. Interestingly, while the PBMC yield and viability were similar using K2EDTA-spray coated or CPT tubes the IFN-γ response of the PBMCs processed via CPT tubes was negatively impacted. We currently do not know the reason for this, but speculate factors such as the high concentration of heparin in the CPT tubes may have negatively impacted downstream cellular responses. While we have not observed this for other species in similar vaccination studies, such a phenomenon may be specifically associated to the rabbit T cell. Until the reason has been defined, we strongly suggest investigators use the processing methodology described in our study.

The ability to assess IFN-γ positive T cell responses against intracellular and microbial pathogen antigens is essential in vaccine development. Vaccines generating strong T cell responses have been associated with preventing or modulating symptoms following infection and clearing infectious diseases such as influenza. In cases such as influenza infection, $CD8^+$ T cells and, in some degree, CD4 + T cells can mediate viral clearance post-infection [25–29]. CD8 + cytotoxic T lymphocytes (CTLs) can recognize and respond to highly conserved internal antigens, such as NP, across influenza subtypes [30] through major histocompatibility complex (MHC) class I presentation pathways and have been implicated in mediating protection against influenza in preclinical models [22,31,32] and human studies [18,19,33,34]. Pre-existing IFN-γ + $CD4^+$ T cells responding to influenza internal proteins resulted in lower virus shedding and less severe symptoms [35]. Our study revealed that vaccination with pNP generated robust cellular immune responses, which were boostable against the influenza NP antigen. This observation was supported by our previous preclinical studies through the demonstration of robust responses to the consensus influenza NP antigen and protective efficacy after heterosubtypic live virus challenge in mice, ferrets, and in non-human primates [22,24].

In addition to the role of IFN-γ T cells in infectious disease, T cell-mediated immunity has also been identified and required in generating systemic antitumor immunity, with MHC class I-restricted IFN-γ + CD8 + CTLs, primarily responsible for mediating tumor killing. As such, IFN-γ + CD8 + T cells that target tumor cells are frequently used to measure vaccine efficacy and also serve as a surrogate endpoint in clinical tumor vaccine trials [36,37]. Adoptive transfer of T cell subsets or *in vivo* depletion have established an important role for CD8 + CTLs in antitumor immunity [38]. Evidence of the substantial role of CD4 + T cells in mediating significant antitumor functions have also been demonstrated [39,40].

Studies are currently ongoing in our laboratory to further define the cellular immune response raised to vaccination in the rabbit, and will be reported at a later date. Flow cytometric tools are being developed so we can monitor the responses of specific T cell subsets, and epitope mapping is ongoing to define the T cell epitopes and possible restriction elements involved in their presentation. Preliminary data suggests a number of immunodominant T cell epitopes to be conserved across this outbred rabbit population. A similar phenomenon has been recently reported in the outbred Hartley guinea pig population [23,41]. Further studies will be required to determine whether non-classical MHC molecules are involved in the presentation of such epitopes.

In our study, we were able to clearly detect cell-mediated immune responses to two different infectious disease vaccines. The development of this assay provides a useful analysis of T cell responses in a translational animal model, which addresses the need for such experimental models in preclinical drug development to study diseases with important T cell components. To this end, progress in developing this relevant animal model for preclinical research will likely reduce the financial and ethical burden of using larger animal models in a growing research field.

Conflict of interest

BSY, HP, AAG, NP, KS, KEB and TRFS are employees of Inovio Pharmaceuticals and receive financial benefits such as salary and own shares or have been awarded stock options in the company. K.M. received grants from Inovio, receiving consulting fees from Inovio related to DNA vaccine development, and a pending patent application (to Inovio) for delivery of DNA-encoded monoclonal antibodies.

Appendix A. Supplementary material

Supplementary data to this article can be found online at https://doi.org/10.1016/j.vaccine.2019.01.006.

References

[1] Fan J, Watanabe T. Transgenic rabbits as therapeutic protein bioreactors and human disease models. Pharmacol Ther 2003;99:261–82.

[2] Bosze Z, Hiripi L, Carnwath JW, Niemann H. The transgenic rabbit as model for human diseases and as a source of biologically active recombinant proteins. Transgenic Res 2003;12:541–53.
[3] Camacho P, Fan H, Liu Z, He JQ. Small mammalian animal models of heart disease. Am J Cardiovasc Dis 2016;6:70–80.
[4] Yanni AE. The laboratory rabbit: an animal model of atherosclerosis research. Lab Anim 2004;38:246–56. https://doi.org/10.1258/002367704323133628.
[5] Cao J, Jager MJ. Animal eye models for uveal melanoma. Ocular Oncol Pathol 2015;1:141–50. https://doi.org/10.1159/000370152.
[6] Del Amo EM, Urtti A. Corrigendum to "Rabbit as an animal model for intravitreal pharmacokinetics: clinical predictability and quality of the published data" [Exp. Eye Res. 137C 111–124]. Exp Eye Res 2015;169 (60):2018. https://doi.org/10.1016/j.exer.2018.01.006.
[7] Duranthon V et al. On the emerging role of rabbit as human disease model and the instrumental role of novel transgenic tools. Transgenic Res 2012;21:699–713. https://doi.org/10.1007/s11248-012-9599-x.
[8] Peng X, Knouse JA, Hernon KM. Rabbit Models for Studying Human Infectious Diseases. Comp Med 2015;65:499–507.
[9] Graur D, Duret L, Gouy M. Phylogenetic position of the order Lagomorpha (rabbits, hares and allies). Nature 1996;379:333–5. https://doi.org/10.1038/379333a0.
[10] Amanna IJ, Slifka MK. Contributions of humoral and cellular immunity to vaccine-induced protection in humans. Virology 2011;411:206–15. https://doi.org/10.1016/j.virol.2010.12.016.
[11] Crotty S. A brief history of T cell help to B cells. Nat Rev Immunol 2015;15:185–9. https://doi.org/10.1038/nri3803.
[12] Darwich L et al. Secretion of interferon-gamma by human macrophages demonstrated at the single-cell level after costimulation with interleukin (IL)-12 plus IL-18. Immunology 2009;126:386–93. https://doi.org/10.1111/j.1365-2567.2008.02905.x.
[13] Mohr E et al. IFN-{gamma} produced by CD8 T cells induces T-bet-dependent and -independent class switching in B cells in responses to alum-precipitated protein vaccine. In: Proceedings of the National Academy of Sciences of the United States of America. p. 17292–7. https://doi.org/10.1073/pnas.1004879107.
[14] Nakajima C et al. A role of interferon-gamma (IFN-gamma) in tumor immunity: T cells with the capacity to reject tumor cells are generated but fail to migrate to tumor sites in IFN-gamma-deficient mice. Cancer Res 2001;61:3399–405.
[15] Overacre-Delgoffe AE et al. Interferon-gamma drives treg fragility to promote anti-tumor immunity. Cell 2017;169. https://doi.org/10.1016/j.cell.2017.05.005.
[16] Sercan O, Stoycheva D, Hammerling GJ, Arnold B, Schuler T. IFN-gamma receptor signaling regulates memory CD8+ T cell differentiation. J Immunol 2010;184:2855–62. https://doi.org/10.4049/jimmunol.0902708.
[17] Tewari K, Nakayama Y, Suresh M. Role of direct effects of IFN-gamma on T cells in the regulation of CD8 T cell homeostasis. J Immunol 2007;179:2115–25.
[18] Hayward AC, Natural T, et al. Cell-mediated Protection against Seasonal and Pandemic Influenza. Results of the Flu Watch Cohort Study. Am J Respir Crit Care Med 2015;191:1422–31. https://doi.org/10.1164/rccm.201411-1988OC.
[19] Sridhar S et al. Cellular immune correlates of protection against symptomatic pandemic influenza. Nat Med 2013;19:1305–12. https://doi.org/10.1038/nm.3350.
[20] McElhaney JE et al. T cell responses are better correlates of vaccine protection in the elderly. J Immunol 2006;176:6333–9.
[21] Lillie PJ et al. Preliminary assessment of the efficacy of a T-cell-based influenza vaccine, MVA-NP+M1, in humans. Clin Infect Dis : Off Publ Infect Dis Soc Am 2012;55:19–25. https://doi.org/10.1093/cid/cis327.
[22] Laddy DJ et al. Heterosubtypic protection against pathogenic human and avian influenza viruses via in vivo electroporation of synthetic consensus DNA antigens. PLoS One 2008;3:. https://doi.org/10.1371/journal.pone.0002517e2517.
[23] Schultheis K et al. Characterization of guinea pig T cell responses elicited after EP-assisted delivery of DNA vaccines to the skin. Vaccine 2017;35:61–70. https://doi.org/10.1016/j.vaccine.2016.11.052.
[24] Laddy DJ et al. Electroporation of synthetic DNA antigens offers protection in nonhuman primates challenged with highly pathogenic avian influenza virus. J Virol 2009;83:4624–30. https://doi.org/10.1128/JVI.02335-08.
[25] Eichelberger M, Allan W, Zijlstra M, Jaenisch R, Doherty PC. Clearance of influenza virus respiratory infection in mice lacking class I major histocompatibility complex-restricted CD8+ T cells. J Exp Med 1991;174:875–80.
[26] Lin YL, Askonas BA. Biological properties of an influenza A virus-specific killer T cell clone. Inhibition of virus replication in vivo and induction of delayed-type hypersensitivity reactions. J Exp Med 1981;154:225–34.
[27] Lukacher AE, Braciale VL, Braciale TJ. In vivo effector function of influenza virus-specific cytotoxic T lymphocyte clones is highly specific. J Exp Med 1984;160:814–26.
[28] Webster RG, Askonas BA. Cross-protection and cross-reactive cytotoxic T cells induced by influenza virus vaccines in mice. Eur J Immunol 1980;10:396–401. https://doi.org/10.1002/eji.1830100515.
[29] Sant AJ, McMichael A. Revealing the role of CD4(+) T cells in viral immunity. J Exp Med 2012;209:1391–5. https://doi.org/10.1084/jem.20121517.
[30] Rimmelzwaan GF, Kreijtz JH, Bodewes R, Fouchier RA, Osterhaus AD. Influenza virus CTL epitopes, remarkably conserved and remarkably variable. Vaccine 2009;27:6363–5. https://doi.org/10.1016/j.vaccine.2009.01.016.
[31] Epstein SL, Lo CY, Misplon JA, Bennink JR. Mechanism of protective immunity against influenza virus infection in mice without antibodies. J Immunol 1998;160:322–7.
[32] Yap KL, Ada GL, McKenzie IF. Transfer of specific cytotoxic T lymphocytes protects mice inoculated with influenza virus. Nature 1978;273:238–9.
[33] McMichael AJ, Gotch FM, Noble GR, Beare PA. Cytotoxic T-cell immunity to influenza. New Engl J Med 1983;309:13–7. https://doi.org/10.1056/NEJM198307073090103.
[34] Wang Z et al. Recovery from severe H7N9 disease is associated with diverse response mechanisms dominated by CD8(+) T cells. Nat Commun 2015;6:6833. https://doi.org/10.1038/ncomms7833.
[35] Wilkinson TM et al. Preexisting influenza-specific CD4+ T cells correlate with disease protection against influenza challenge in humans. Nat Med 2012;18:274–80. https://doi.org/10.1038/nm.2612.
[36] Ogi C, Aruga A. Immunological monitoring of anticancer vaccines in clinical trials. Oncoimmunology 2013;2:. https://doi.org/10.4161/onci.26012e26012.
[37] Hoos A et al. Improved endpoints for cancer immunotherapy trials. J Natl Cancer Inst 2010;102:1388–97. https://doi.org/10.1093/jnci/djq310.
[38] Melief CJ. Tumor eradication by adoptive transfer of cytotoxic T lymphocytes. Adv Cancer Res 1992;58:143–75.
[39] Dranoff G et al. Vaccination with irradiated tumor cells engineered to secrete murine granulocyte-macrophage colony-stimulating factor stimulates potent, specific, and long-lasting anti-tumor immunity. PNAS 1993;90:3539–43.
[40] Hung K et al. The central role of CD4(+) T cells in the antitumor immune response. J Exp Med 1998;188:2357–68.
[41] Gillis PA et al. Development of a novel, guinea pig-specific IFN-gamma ELISPOT assay and characterization of guinea pig cytomegalovirus GP83-specific cellular immune responses following immunization with a modified vaccinia virus Ankara (MVA)-vectored GP83 vaccine. Vaccine 2014;32:3963–70. https://doi.org/10.1016/j.vaccine.2014.05.011.